Landsc Ecol (2025) 40:189
https://doi.org/10.1007/s10980-025-02200-2

RESEARCH ARTICLE

UAS and high-resolution satellite imagery improve the accuracy of cheatgrass detection across an invaded Yellowstone landscape

Jason Kreitler · Josh von Nonn · Seth Munson · Alex C. Zaideman · Steven T. Bekedam · Ann Rodman · Miguel L. Villarreal

Received: 27 December 2024 / Accepted: 6 August 2025 / Published online: 3 October 2025
This is a U.S. Government work and not under copyright protection in the US; foreign copyright protection may apply 2025

Abstract

Context Cheatgrass (*Bromus tectorum* L.) is a problem across the western United States, where it outcompetes and replaces native grass species, alters habitats, and increases the risk of wildfires. Cheatgrass greens up earlier in the growing season compared to native grasses, making it classifiable with multi-temporal and multi-spectral remote sensing.

Objectives We mapped cheatgrass at different scales in the Greater Yellowstone Ecosystem using 10-m Sentinel-2 imagery, 3-m PlanetScope, and 10-cm Uncrewed Aerial Systems (UAS) imagery. We compared these maps to field-collected data to address 1) variation in seasonal phenological signals of native and cheatgrass patches, 2) the influence of scale on detectability and map accuracy across our study area.

Results Model accuracy to predict cheatgrass presence increased with imagery resolution and ranged from 83% using 10-m Sentinel-2 to 94% with the integration of PlanetScope and UAS imagery. While there was spatial agreement across models, the fusion of UAS data with satellite sources allowed the detection of small cheatgrass with more precision. Our novel use of NExR and dNExR (a redness and differenced redness index) data in the classification of cheatgrass capitalizes on the senescence of cheatgrass during peak summer periods where cloud free imagery is more prevalent.

Conclusions Our satellite and UAS-based models of cheatgrass prediction compare the fusion of very high resolution imagery and phenological time differencing to identify infested areas. Tradeoffs between accuracy and expense lead to important questions for management applications.

Keywords *Bromus tectorum* · Cheatgrass · Remote Sensing · UAS · Yellowstone · Satellite · Sentinel-2 · PlanetScope

Supplementary Information The online version contains supplementary material available at https://doi.org/10.1007/s10980-025-02200-2.

J. Kreitler (✉)
U.S. Geological Survey, Western Geographic Science Center, 230 Collins Rd, Boise, ID 83702, USA
e-mail: jkreitler@usgs.gov

J. von Nonn · M. L. Villarreal
U.S. Geological Survey, Western Geographic Science Center, P.O. Box 158, Moffett Field, CA 94035, USA

S. Munson
U.S. Geological Survey, Southwest Biological Science Center, 2255 N. Gemini Dr, Flagstaff, AZ 86001, USA

A. C. Zaideman · S. T. Bekedam · A. Rodman
National Park Service, Yellowstone National Park, P.O. Box 168, Yellowstone NP, WY 82190, USA

Introduction

Invasive grasses pose a large threat to ecosystems and can require considerable costs to control and

eradicate infestations (D'Antonio and Vitousek 1992; BenDor et al. 2015). Cheatgrass (*Bromus tectorum* L.) is a non-native invasive annual grass introduced from Eurasia that has spread to millions of hectares across the western U.S. and other regions globally (Mack 1981). Cheatgrass can transform ecosystems due to its rapid growth and fecundity (Mack and Pyke 1983) that allow the invasive to suppress native species (Booth et al. 2003). Increases in its dominance within plant communities is further enhanced from the proliferation of fine fuels that can lead to a positive invasive grass-wildfire feedback cycle (D'Antonio and Vitousek 1992; Balch et al. 2013). Early detection and monitoring of cheatgrass is critical to slow its spread and reduce negative impacts to ecosystems (Bradley 2014). The Greater Yellowstone Ecosystem (GYE) represents one of the most intact ecosystems in North America that is valued for its abundant wildlife, diverse plant communities, cultural resources, and essential ecosystem services (Keiter and Boyce 1994). The landscape has also been intensively managed to conserve these resources, including within the world's first national park, Yellowstone National Park, adjoining Grand Teton National Park, National Elk Refuge, and surrounding national forests. While many invasive species have encroached on the GYE, cheatgrass is one of the more recent and pervasive threats facing the region (Barnett et al. 2007). The abundance of invasives in the GYE has increased over the past several decades and has required a growing number of resources to reduce and potentially eradicate them from managed areas (Olliff et al. 2001). Initial cheatgrass spread is largely limited to lower elevation reaches of the GYE landscape on dry, south- and east-facing slopes (Peeler and Smithwick 2018), while many of the higher elevation forest areas have cold temperatures and a short growing season that limit cheatgrass germination (Terry et al. 2024) and establishment (Bradford and Lauenroth 2006). Where present, many areas within the GYE are at an early stage of cheatgrass invasion, when small investments can potentially limit its spread. However, cheatgrass has expanded into higher elevations over the past decades in the Great Basin (Smith et al. 2022), and climate change and resultant shifts in plant distributions can create new opportunities for cheatgrass invasion in previously uninvaded areas (Bradley 2009; Sofaer et al. 2022).

To limit the further advancement of cheatgrass and other invasive grasses, new tools and technologies are needed to provide early detection and surveillance of invasive spread and to guide management actions. Remote sensing products, including from satellite and airborne platforms, have been instrumental to expanding the spatial and temporal extent of invasive detection and monitoring (Huang and Asner 2009). Remote sensing can provide near-real time estimates of cheatgrass invasion patterns over broad spatial extents compared to resource intensive plot-based monitoring. Past remote sensing-derived cheatgrass and annual grass classifications, including those from the Rangeland Analysis Platform (https://rangelands.app/rap) and RCMAP (Rangeland Condition Monitoring, Assessment, and Projection; Rigge et al. 2020), often interpolate cheatgrass occurrence and abundance with sparsely distributed datasets that are not trained with data from a focal area of interest. Furthermore, many available invasive species tools lack sufficient resolution or sensitivity to capture early patterns of invasion that can inform land management.

Invasive grasses often occupy unique niches and exhibit priority effects that allow them to remain in distinct spaces and periods of time compared to native species (Wolkovich and Cleland 2011). Cheatgrass has different phenology patterns compared to native vegetation, often producing an early and distinctive pulse of "greenness" in the early spring that can be detected using multispectral satellite data (Singh and Glenn 2009; Boyte et al. 2015). This signal can be used to map cheatgrass by differencing a spring image (or image composite) capturing peak cheatgrass greenness and a later summer image where cheatgrass is senescent and native vegetation is at peak greenness (Kokaly 2010a; Bishop et al. 2019; Villarreal et al. 2019). Despite this proven approach, previous efforts have relied on moderate resolution Landsat satellite imagery (30 m) that is used for generating probabilities of cheatgrass occurrences but is less effective in pinpointing smaller patches when an infestation is early in its invasion and can be more easily eradicated from a region (Leung et al. 2002). This phenologically based remote sensing approach is effective in mapping cheatgrass and other invasive species in arid parts of the western U.S. (Pastick

et al. 2020; Smith et al. 2023), though it may not be as suitable for the GYE due to excessive cloud and snow cover in the spring and early summer that complicate efforts to find quality satellite observations or for detecting low density patches that are intermixed with native vegetation.

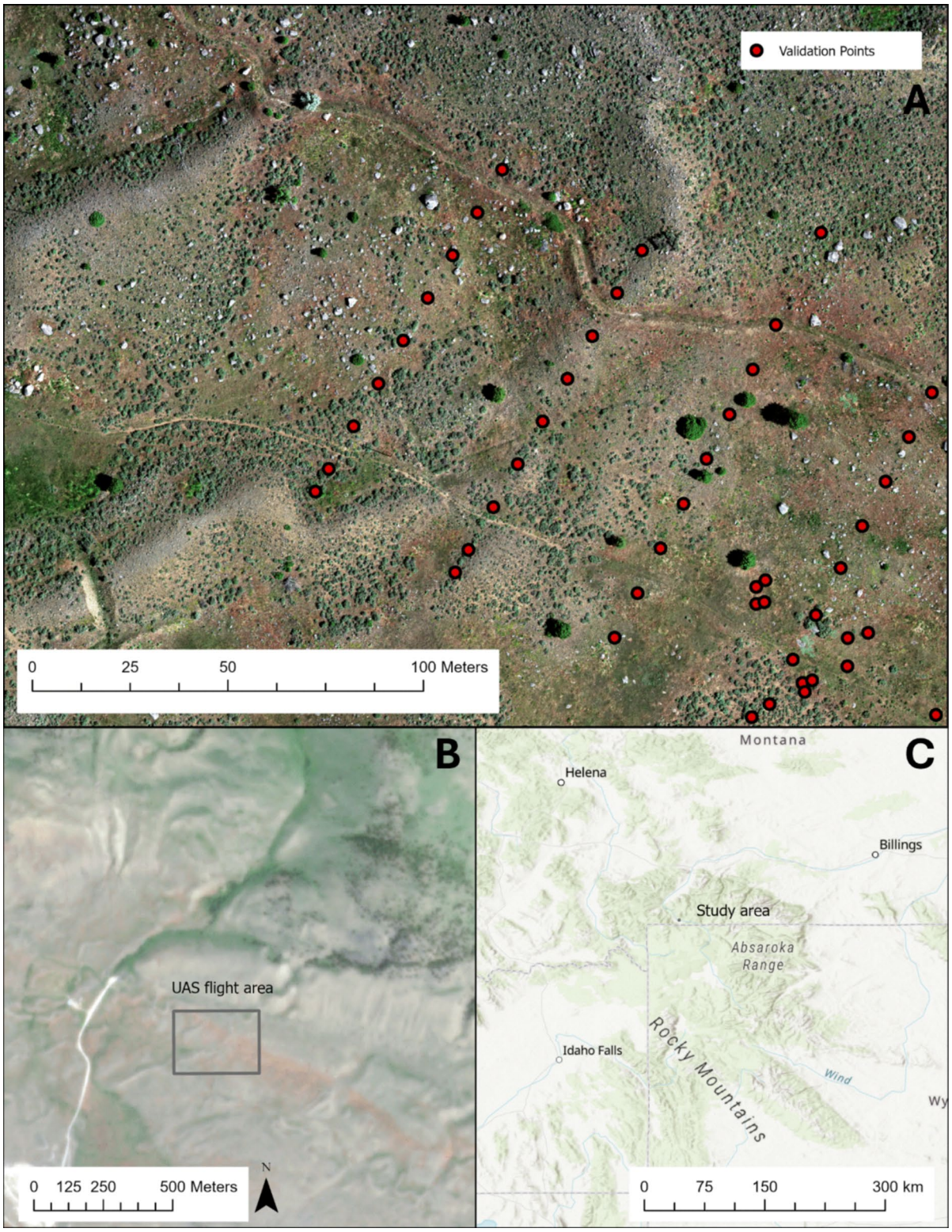
Uncrewed aerial systems (UAS) show great promise in increasing the resolution and accuracy of detecting invasive species and monitoring their spread (Zhou et al. 2023; Singh et al. 2024). UAS can also be cost-effective and offers flexibility in survey timing and sensor use (reviewed in Singh et al. 2024). The application of UAS-based remote sensing for identifying invasive plants is rapidly increasing in research and applied use. For example, using high-resolution RGB imagery, Sandino and Gonzalez (2018) demonstrated that buffelgrass (*Cenchrus ciliaris* L.) and spinifex (*Triodia* sp.) can be accurately classified; Elkind et al. (2019) trained WorldView-2 satellite imagery with high-resolution (12 cm) UAS imagery to detect buffelgrass across Saguaro National Park in Arizona; Nascente et al. (2022) successfully used image segmentation and classification of multi-date UAS imagery to map invasive drooping forkedfern (*Dicranopteris flexuosa* Schrad.) following prescribed burning; Zhu et al. (2019) used multi-temporal UAS imagery to capture spatio-temporal dynamics and investigate drivers of smooth cordgrass (*Spartina alterniflora* Loisel.) expansion at both patch and landscape scales; and Bishop and Errigo (2023) mapped cheatgrass litter in the Mojave Desert with high accuracy; however, accuracy was variable across study sites and influenced by soils and topographic variability. Most similar to our study was Weisberg et al. (2021), who demonstrated that having multitemporal RGB imagery was more important than a near-infrared band in detecting cheatgrass in the Great Basin. This finding differs from many Landsat-based remote sensing studies of cheatgrass that use a phenological signal from a normalized difference vegetation index (NDVI) to accurately classify invaded areas (Kokaly 2010a; 2010b; Waller et al. 2018; Villarreal et al. 2019).

The growth of UAS applications in landscape ecology, in particular the ability to detect target species at fine scales and the potential to fuse UAS with image sources of different resolutions to predict across large landscapes, has vegetation managers interested in its application to their problems with cheatgrass (Villarreal et al. 2025). There is a need for leveraging remote sensing data at a variety of scales to first identify possible areas of infestation across large landscapes and precisely inventory high probability sites to cost-effectively prioritize remediation or treatment actions. To inform the development of invasive species detection and monitoring across broad landscapes, the objectives of this research were to (1) test UAS-based remote sensing to accurately map cheatgrass, (2) understand tradeoffs in image resolution and multi-temporal observations for accurate detection of cheatgrass, and (3) provide guidance to land managers on the application of these methods to address their vegetation and invasive species management decision making.

Methods

Study area

Our study site was a 10 ha area in the US Forest Service Hayes Pasture near Gardiner, MT, near the northern gate to Yellowstone National Park (Lat 45° 3.0' N, Lon 110° 41.8' W, Fig. 1). The area receives 25 cm of mean annual precipitation (Billings, MT Weather Forecast Office 2024) and sits on a hillside gradient from 1910 to 1870 m elevation of poorly developed soils classified as agric cryoborolls and typic cryoborolls of glacial origin (Soil Survey Staff, NRCS, USDA 2025). The site has a prominent southern exposure that gradually slopes to a smooth brome (*Bromus inermis* Leyss.) dominated pasture. The hillside vegetation is primarily composed of big sagebrush (*Artemisia tridentata* Nutt.) and associated species like rabbitbrush (*Chrysothamnus* Nutt.), Rocky Mountain juniper (*Juniperus scopulorum* Sarg.), and Columbia needlegrass (*Achnatherum nelsonii* Scribn.). Cheatgrass is the primary invasive species present in patches ranging from large infestations to low percent-cover infestations mixed in with sagebrush and other native species, or within an assemblage of other non-native species including desert alyssum (*Alyssum desertorum* Stapf), tansymustard *(Descurainia sp.)*, and common mullein (*Verbascum thapsus* L.) An abandoned irrigation canal lies near the top of the study area and where vegetation is most 'departed' from a more natural condition. A landscape photograph is


Validation Points
A
0 25 50 100 Meters
B
UAS flight area
0 125 250 500 Meters
N
C
Montana
Helena
Billings
Study area
Absaroka Range
Rocky Mountains
Idaho Falls
Wind
Wy
0 75 150 300 km

◂**Fig. 1** UAS flight area near Gardiner, MT, USA. Imagery in the top pane (A) is from the MicaSense sensor, with RGB bands mapped to true color. The July 15th, 2022, PlanetScope scene in the lower left (B) is also mapped with RGB bands to true color. The study area is shown in panel C

provided in the supplement to show typical vegetation, slope, and aspect of the study area (Figure S1).

UAS data collection -

We conducted two UAS flights on July 12th, 2023, at the Gardiner, MT study site (Fig. 1) with a 3DR Solo quadcopter (3DR, Chula Vista, CA, USA): the first captured the visible spectrum (RGB) using a Ricoh GR III camera (Ricoh, Tokyo, Japan), and the second captured multispectral imagery (MS) with a MicaSense RedEdge-M sensor (Micasense, Seattle, WA, USA). Both flight plans were created using Mission Planner (ver. 1.3.68) with parallel East–West transects providing optimal pixel coverage for scaling to satellite (Chintanadilok et al. 2022). We flew the RGB sensor at 60 m above-ground-level (AGL) with 80% front and side overlap in the nadir position, while the MS sensor was flown at 60 m AGL with 85% front and side overlap in the nadir position. Five ground control points (GCP) were evenly distributed across the site and geolocated with an Emlid M2 GNSS receiver (Emlid, Budapest, Hungary) mounted on a 2 m survey rod using Emlid Survey (Emlid Ltd 2024). GCP points were processed in Emlid Studio to provide post-processed kinematic sub-centimeter precision using a nearby Emlid RS2 + base station. We processed the RGB imagery in WebODM (ver. 2.1), resulting in a 3 band 1.2 cm ground sampling distance (GSD) orthomosaic, and processed the MS imagery with the MicaSense radiometric calibration panel data using Metashape (ver. 1.8) to produce a 5 band, 4.3 cm GSD orthomosaic (WebODM Authors 2024; Agisoft LLC, 2023). Multispectral bands included blue (475 nm center), green (560 nm center), red (668 nm center), red edge (717 nm center), and near infrared (842 nm center). Coregistering, or spatially aligning, the MS imagery with the RGB was performed in QGIS (ver. 3.22) for imagery analysis (QGIS.org 2024). We resampled both datasets to 10 cm from their native resolution to reduce file size.

UAS and satellite model validation data

Prior to the UAS flights, we placed sixteen 50 × 50 cm quadrats and performed an ocular estimate of vegetation composition and cheatgrass percent cover within seven bins: not present, 1–5%, 6–15%, 16–25%, 26–50%, 51–75%, and 76–100%. We located quadrats to capture variation in cheatgrass distribution and other representative vegetation types. We marked quadrat corners using an Emlid Reach M2 with 1 cm accuracy. Within the UAS flight area, we also collected validation data along four 100 m long transects running up slope, spaced 40 m apart, and generally bisecting the primary area of dense cheatgrass infestation (Fig. 1). We tried for 10 points on each transect, with the observer estimating percent cheatgrass cover in a 1-m radius area around each point, taking a nadir photograph and recording GPS coordinates. Due to obstacles on the transects, we ended with 37 validation points from the transects and sampled 16 quadrats leading to 53 independent validation points for accuracy assessment of our classified models (Fig. 1; Kreitler et al. 2025).

UAS and satellite model training data

We collected three additional types of training and field data to capture different information about cheatgrass and paired control sites (similar and adjacent uninvaded natural vegetation) at scales relevant to satellite and UAS data. Field data collection followed a protocol developed specifically for our land management partners to map cheatgrass in the GYE. Field crews were instructed to target small to large areas with low to high canopy cover of cheatgrass and map cheatgrass across a range of elevation, climate, plant and soil types. The protocol is a 14-step process for field personnel to record the precise location and important attributes of the patches (i.e., percent cover, phenology, coordinates). We developed an application using Esri FieldMaps (Esri, Redlands, California) to record location and log data on a GPS enabled tablet or phone. These entries are then uploaded to a central National Park Service (NPS) field collection database for use in later analyses. Within our UAS flight area, we recorded 10 polygons of cheatgrass and control

areas (non-invaded vegetation) with a high-resolution GPS receiver (10 cm accuracy).

To identify and define periods of peak cheatgrass greenness and senescence to drive our phenological understanding, we digitized distinctive patches of dense cheatgrass and native vegetation from the July 15, 2022, PlanetScope scene near Gardiner, MT. The cheatgrass patches in this area are well established and well known to local vegetation managers. We digitized patches large enough to capture a strong phenological signal from cheatgrass or paired uninvaded control plots (Fig. 2). In addition to the commonly used differenced normalized difference vegetation index (dNDVI), we investigate the use of a multi-temporal redness index to capture differences in the visible spectrum between cheatgrass and native plants during the late season when cloud-free images are more abundant. We calculated the Excess Red Vegetation Index (NExR; Meyer et al. 1999; Meyer and Neto 2008), based on the red and green band as: 1.4R -G, which was normalized as NExR = (1.4R-G)/(1.4R + G). The differenced NExR (dNExR) is the difference between the early season NExR and late season NExR. Likewise, we calculate dNDVI using early and late season NDVI. Using the digitized patches of cheatgrass and native vegetation, we plot the patch mean values of Sentinel-2 derived NDVI and NExR over the 2022 growing season to determine the dates of maximum difference between cheatgrass and paired native patches (yellow lines in Fig. 2) to generate a dNDVI and dNExR data layer from Planet and Sentinel-2 imagery with those derived dates (Fig. 2).

Using the 10 cm resolution RGB UAS imagery, we generated a binary (presence/absence cheatgrass) training dataset (n = 363) within our UAS flight area (Fig. 1). We hand digitized cheatgrass presence training data in Google Earth Engine (GEE, Gorelick

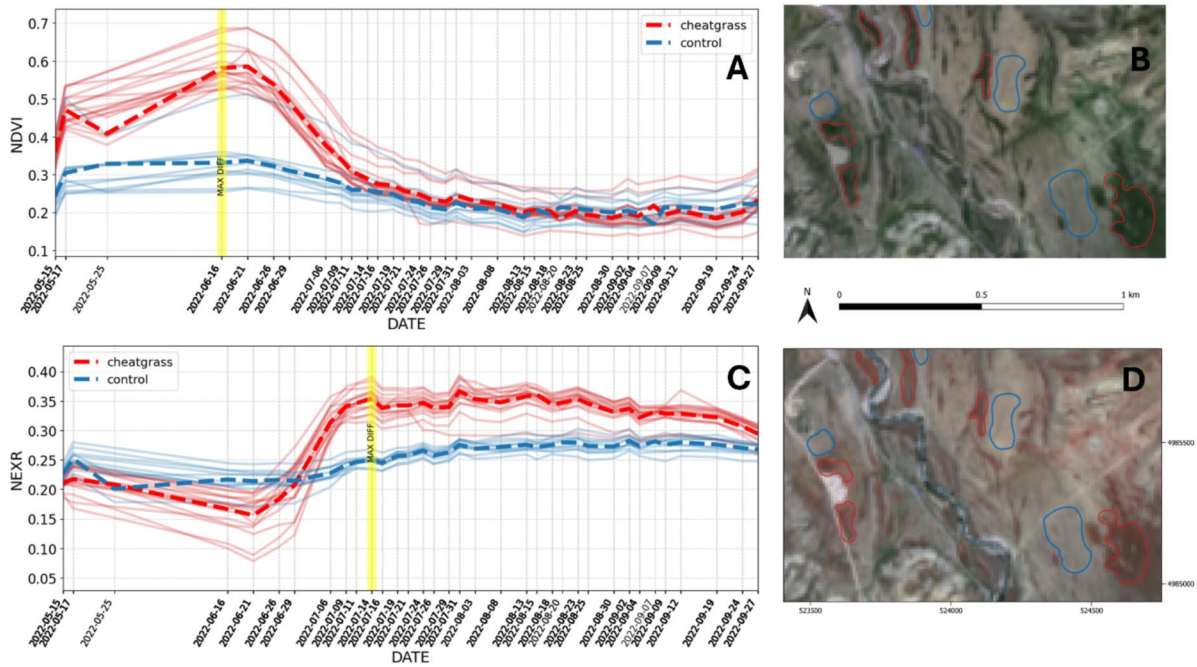


Fig. 2 Seasonal time series of normalized difference vegetation index (NDVI—A) and normalized excess red index (NExR—C) for 2022 from Sentinel-2 imagery. Red and blue lines in the graphs show the time series for cheatgrass and uninvaded vegetation control sites, respectively. The dashed red and blue lines represent the mean of observations. Polygons in the imagery examples (B and D) correspond to cheatgrass and uninvaded vegetation control training sites. The imagery in B is from June 22nd, 2022, while the imagery in D is from July 15th, 2022. The vertical yellow lines represent the maximum differences between cheatgrass and control plots and are used as the dates for dNDVI and dNEXR analyses

et al. 2017) using the 10 polygons of cheatgrass and control locations, our extensive knowledge of the vegetation of the flight area, and the location of predominant cheatgrass patches, which were observable in the 10 cm imagery. Likewise, with the high-resolution UAS imagery, we distributed absence points across the various visible vegetation types, including sagebrush (*Artemisia* L.), small trees, and other perennial vegetation, and abiotic features to guide classification models using a wide variety of signals that were not cheatgrass. These methods were similar to Elkind et al. (2019) and Weisberg et al. (2021), who also generated training data from very high resolution (2–12 cm) UAS-derived RGB imagery.

Planet and Sentinel-2 data imagery analysis

Using the sequence of cloud-free Sentinel-2 imagery (European Space Agency 2024), we identified the date of maximum difference between 10 cheatgrass and control polygons for NDVI and NExR values over the 2022 growing season in an area around Gardiner, MT (Fig. 2). Identifying these periods of important peaks of cheatgrass phenology allowed us to choose specific periods to use in creating dNDVI and dNExR data layers using PlanetScope and Sentinel-2 imagery for our classification models. We include data from 2022 because an atmospheric river event in June led to a late-spring and above-average precipitation resulting in catastrophic flooding of the Gardiner and Yellowstone Rivers, and subsequent damage to the town of Gardiner and infrastructure in Yellowstone National Park. This weather event and the prevailing weather conditions also resulted in a very productive growing season for cheatgrass, evident in the strong signal in satellite imagery. We acquired 2023 PlanetScope and Sentinel-2 imagery to produce dDNVI and dNExR data using the same methodology of finding peak differences between cheatgrass and control polygons.

We downloaded multiband PlanetScope imagery for June 22nd and July 13th, 2022, and June 6th and July 13th, 2023, as the best available cloud-free dates for peak greenness and senescence in our study area through time series analysis (as in Fig. 2). We queried the Planet API and used Planet's clip, harmonize (to Sentinel-2 imagery), and coregister tools to download the 8-band orthorectified surface reflectance product (Planet Labs PBC 2022). This final step produced image pairs with tight coregistration to allow time series differencing to produce the dNDVI and dNExR data layers. In GEE we queried Sentinel-2 data from the Level-2A orthorectified and atmospherically corrected surface reflectance data to correspond with our cheatgrass green-up and senescence timing. We linked cloud mask data in GEE (Cloud Score + Pasquarella et al. 2023) to further refine our Sentinel-2 data to ensure cloud, haze, and cloud shadow free imagery. Finally, we uploaded our UAS derived imagery (MS and RGB) to GEE for analysis and classification.

Image classification and modeling

To address our questions of how spatial resolution affected our ability to detect cheatgrass, we constructed models with Sentinel-2 data (10 m), PlanetScope data (3 m), and we paired both Sentinel-2 or PlanetScope scenes individually with UAS-derived imagery (10 cm; Kreitler et al. 2025), resulting in four independent models of varying resolution to evaluate. Through exploratory model development, we found the variables dNDVI, dNExR, June NDVI, July NExR, and slope explained most of the variation in the training/testing data as evidenced by variable importance (Table 1) and model accuracy. We substituted UAS-derived variables (July NExR and July NDVI) with Sentinel-2 or PlanetScope derived NExR or NDVI layers in the base models to test the effect

Table 1 Model specification and variable importance (% importance) from the Random Forest classification. Source is the satellite or UAS platform (Sentinel-2, Planet, Sentinel-2 + UAS, Planet + UAS: models 1–4, respectively). For Models 1 and 2, NDVI is from June. For Models 3 and 4, NDVI is UAS-based from the July flight. Variables dNDVI and dNExR are differenced from June and July satellite imagery sources

	Model			
	1	2	3	4
Source	Sentinel-2	Planet	Sentinel-2 + UAS	Planet + UAS
Variable	Importance			
dNDVI	16.88	18.39	18.82	20.39
NDVI	21.88	20.46	19.69	18.78
dNExR	14.40	14.43	19.14	18.99
NExR	22.60	23.15	22.41	22.19
Slope	24.24	23.56	19.94	19.65

of adding single date high resolution UAS imagery to models (Table 1).

To classify images, we used the Random Forest classifier (Breiman 2001) in GEE (Gorelick et al. 2017). Random Forest (RF) is a common machine learning classification method that creates many decision trees and then through 'voting', determines the best ensemble to minimize variance within the model. RF models are often used in this type of remote sensing analysis and are computationally efficient compared to more sophisticated models (Maxwell et al. 2018). In our RF implementation, we parameterized our model using 100 trees, a minimum leaf population of 2, and the remaining parameters as defaults including a bag fraction of 0.5, variables per split as the square root of the number of variables, and unlimited max nodes. We evaluated each model's performance and accuracy in a confusion matrix comparing predicted values to an independent validation dataset. To compare the output of each model we generate the following landscape metrics in R (v4.4.0; R Core Team 2024): total area, mean patch size, median patch size, number of patches, and edge density, using the Landscapemetrics package (v2.1; Hesselbarth et al. 2019). These metrics provide summary statistics valuable for interpreting the patchiness and shape of the model results and provide a complement to the accuracy assessment presented.

Table 2 Landscape and patch metrics of binary classified cheatgrass from models 1–4

	Total Area (ha)	Mean Patch Size (ha)	Median Patch Size (ha)	# Patches	Edge Density
Model 1	1.88	1.34E-01	1.00E-02	21	451.61
Model 2	2.70	1.69E-01	1.89E-02	23	471.59
Model 3	2.07	4.36E-05	2.00E-06	85,764	23,610.32
Model 4	2.08	3.46E-05	1.00E-06	110,351	24,869.68

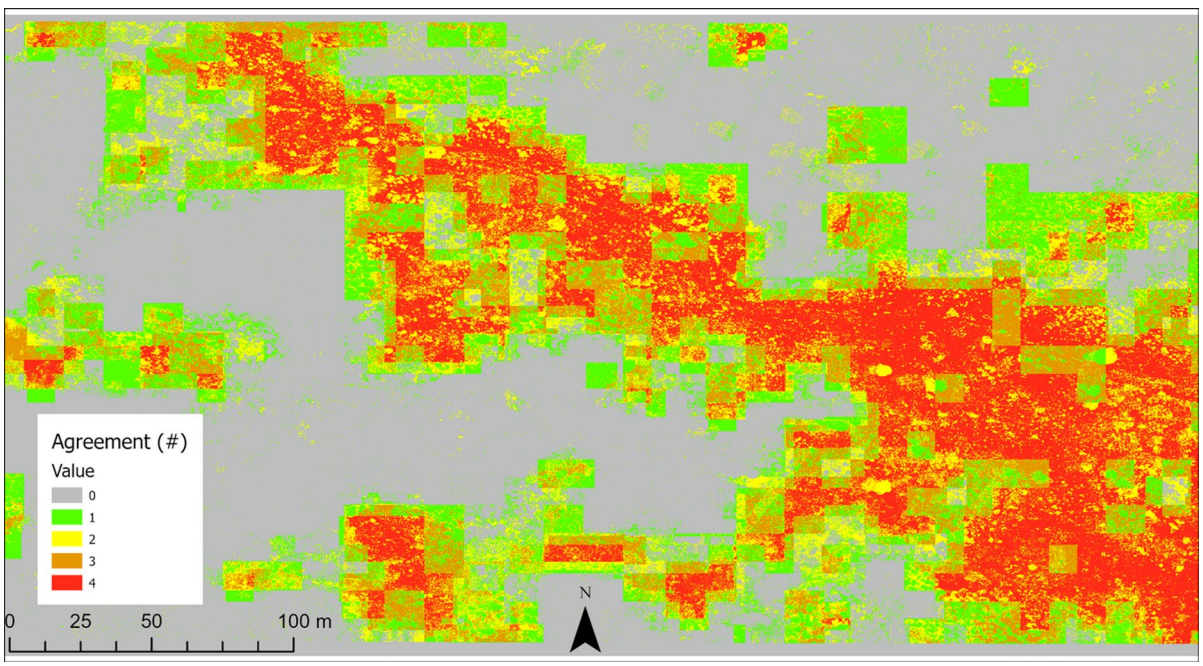


Fig. 3 Model agreement (# of models) of predicted cheatgrass presence from the 4 models. A value of 4 means perfect agreement with each model predicting presence at that pixel. A value of 1 means only one model predicted cheatgrass presence at that pixel, and 0 indicates no model predicted presence at that pixel

Results

Our random forest classification models predicted between 1.88 and 2.70 ha of cheatgrass in our 10-ha study area (Table 2). Comparing across models, the general location of cheatgrass is similar (Fig. 3) and indicates some spatial agreement of cheatgrass location in many areas. However, the effect of increasing resolution is evident in the size of patches produced and the level of detail, both a function of the pixel resolution of imagery sources (Figs. 4 and 5, Table 2). The effect of increasing resolution is also observable in the calculated landscape metrics for each model (Table 2); we see a general split in the landscape metrics between models 1 and 2 compared with models 3 and 4, due to the use of fine scale (10 cm) UAS data (Table 2). Most notable is the increase in total number of patches, decrease in patch size, and increase in edge density when using UAS data compared to Sentinel-2 or PlanetScope data (Table 2 and visually in Fig. 5). Also notable is the similarity in landscape metrics between models using Sentinel-2 and PlanetScope data.

Overall accuracy of the four models ranged from 83 to 94% and increased with finer resolution input data (Table 3); models with PlanetScope data were more accurate than models with Sentinel-2 data, and each model fused with a combination of UAS and satellite data was more accurate than its counterpart (Table 3). In each comparison with validation data and model output, false positives outnumbered false negatives (Table 3). In the models with UAS data (model 3 and 4), the detail is fine enough to differentiate individual trees, boulders, and even large sagebrush crowns in the model outputs (Fig. 4). This distinction allows the model to more accurately pinpoint cheatgrass by removing vegetation or other classes, where in coarser resolution models, they are conflated in mixed pixels.

The differences in percent variable importance among each spectral and topographic explanatory variable to explain cheatgrass presence did not substantially change among models (Table 1). The

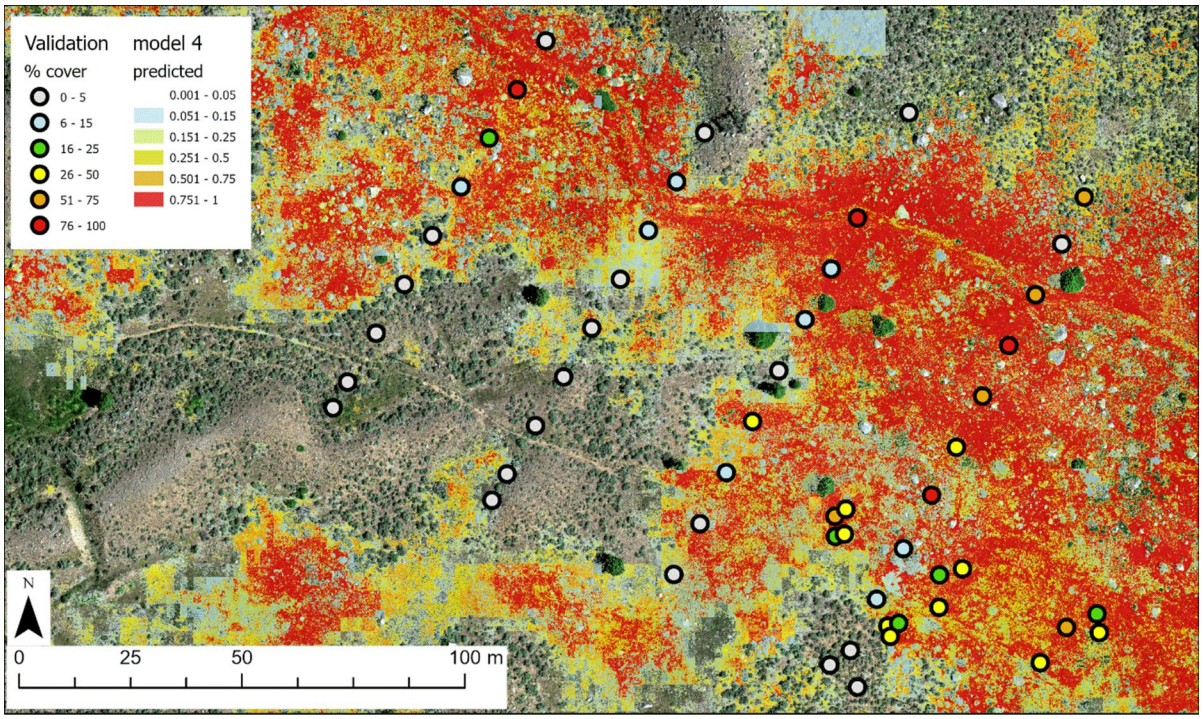


Fig. 4 Random Forest model 4 (PlanetScope + UAS) result draped over UAS imagery (10 cm) and centered around validation points to illustrate the detail and ability to differentiate vegetation types. Validation points represent the percent cover of cheatgrass observed at each point, while the model result maps the prediction of occurrence at each pixel

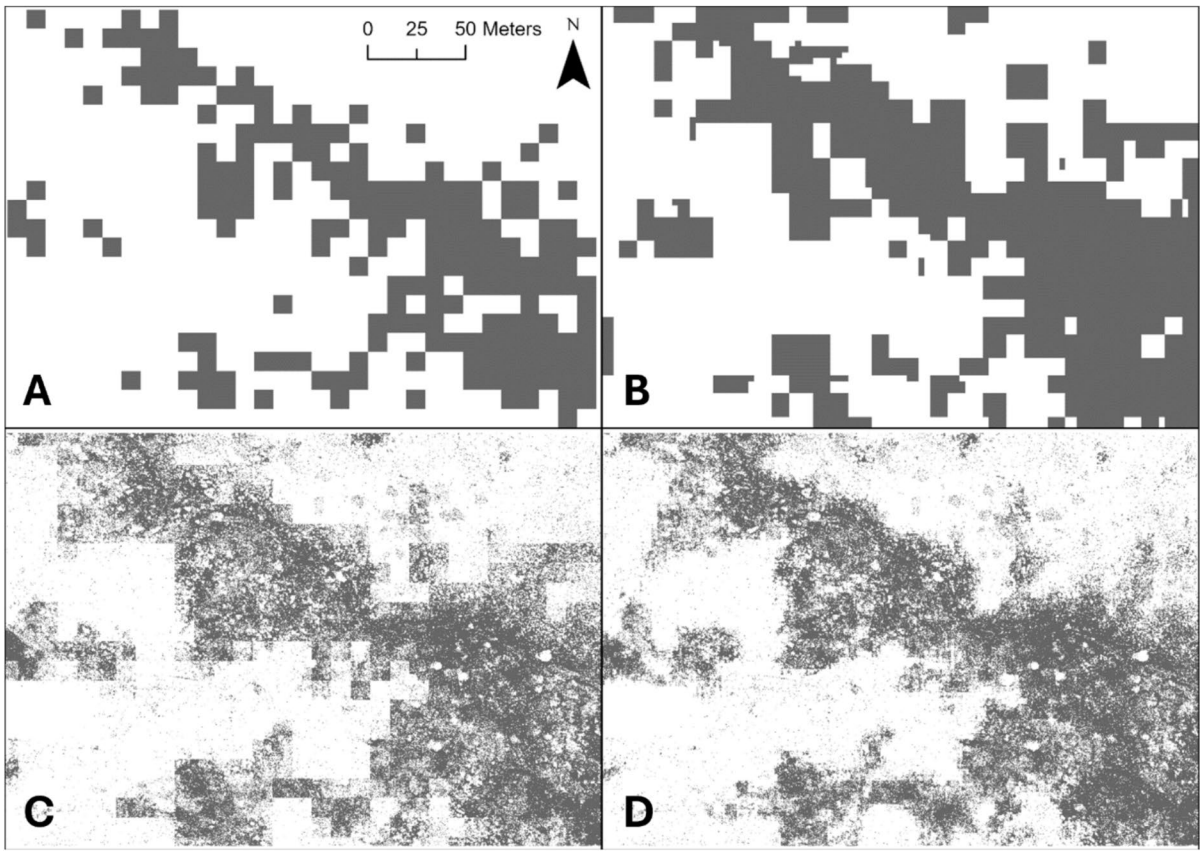


Fig. 5 Binary presence (grayscale, probability > 0.25) of modeled cheatgrass for model 1 using Sentinel-2 imagery (A), model 2 using PlanetScope imagery (B), model 3 using Sentinel-2 and UAS (C), and model 4 using PlanetScope and UAS imagery (D)

Table 3 Confusion matrices showing the accuracy for the four models (Sentinel-2, Planet, Sentinel-2 + UAS, Planet + UAS: models 1–4, respectively)

	Model 1			Model 2			Model 3			Model 4		
	0	1		0	1		0	1		0	1	
0	14	7		0	15	6	0	17	4	0	19	2
1	2	30		1	1	31	1	1	31	1	1	31
Accuracy			83%			87%			91%			94%

Table 4 Spatial intersection over union matrix showing the pairwise similarity of model results.

Model	1	2	3	4
1	1.00			
2	0.49	1.00		
3	0.46	0.51	1.00	
4	0.48	0.48	0.72	1.00

percent variable importance only varied about 4% for models 3 and 4, and up to 10% in model 1. NExR was the most important variable in models 2–4. There was some variation in the similarity of where models predicted the spatial occurrences of cheatgrass (Table 4) – the highest similarity (0.72) was between model 3 and 4, showing the importance the spatial resolution of UAS data for those models. For other

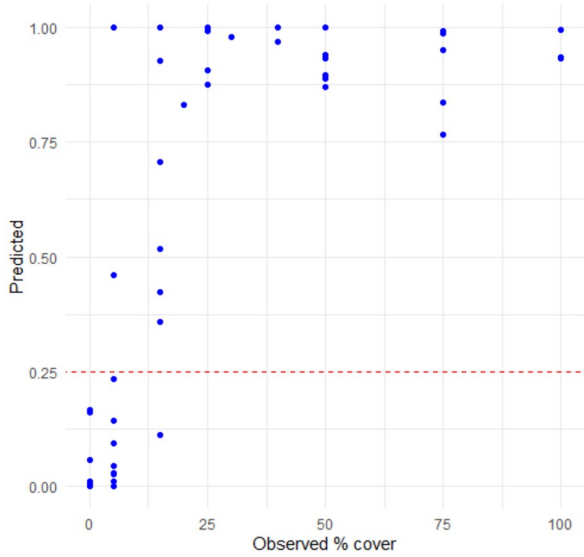


Fig. 6 Predicted probability of cheatgrass detection for model 4 (PlanetScope + UAS) compared with observed cheatgrass percent cover at validation points. Dashed red line is the 0.25 threshold for a predicted presence

combinations, similarity, calculated as the intersection over union (IOU), ranged between 0.46 and 0.51 (Table 2), indicating the agreement between two models (their intersection) was about half of their combined predicted area. The detection of small cheatgrass patches and evidence of fine scale spatial heterogeneity is evident and demonstrates the effect of including the high resolution UAS data (Fig. 3, Table 2).

Model 4 (Planet + UAS) was our most accurate model in predicting cheatgrass and effectively classified low levels of cheatgrass percent cover (Fig. 6). The relationship between observed percent cover and modeled probability indicates a tight clustering of low percent cover values and low probability. Then, the probability increases quickly and begins to plateau around 30% observed cheatgrass cover, with decreasing variability of modeled probability at higher level of observed percent cover. This relationship is similar for all models with the primary difference of model 4 having fewer false positives (2) compared with the other models (4–7), and a lower spread or variation of predicted estimates over the range of observed cover (Figure S3).

The considerable interannual variability of data important for explaining cheatgrass between the years 2022 and 2023 that we observed was both a function of available imagery and the plant's response to environmental conditions. To address variability, we produced combined 'max' dNDVI and dNExR images that took the pixel-wise maximum of dNDVI and dNExR over two seasons. Our study area was not treated with herbicide or other means to reduce cheatgrass; therefore, we expect the distribution to be relatively constant over this short period.

Discussion

We mapped cheatgrass at 83–94% accuracy by integrating satellite and UAS imagery across a partially modified landscape infested by cheatgrass and other invasive species. Our models were able to detect small cheatgrass patches with higher accuracy than larger-scale approaches that use sparse field-data and/or moderate resolution imagery like RAP (Allred et al. 2021) and RCMAP (Rigge et al. 2020) which can accurately estimate west-wide rangeland cover components but are less accurate when high-resolution data are required to prioritize local management actions. Independent of UAS data, our phenological differencing of PlanetScope or Sentinel-2 imagery to distinguish cheatgrass from native vegetation can be used in a regional context to scale up beyond our UAS study site.

Capturing phenology

Flying UAS provides the flexibility to sample when desired phenological conditions exist and to be less

influenced by cloud cover occluding satellite overpasses (Weisberg et al. 2021; Villarreal et al. 2025). One opportunity for future improvement of UAS data collection efforts is to include multiple UAS flights and time series imagery to allow the production of very high resolution dNDVI and dNExR data similar to our use of PlanetScope and Sentinel-2 imagery (Fig. 2), instead of single date UAS imagery, if time and budgets allow. Weisberg et al. (2021) flew their UAS eight times during their study; however, in practice this is likely an unreasonable outlay of resources. This study shows a single UAS flight, coupled with PlanetScope or Sentinel-2 imagery, can capture cheatgrass phenology and high spatial resolution without repeat flights. Capturing cloud-free imagery in mountainous terrain during late spring/early summer can be a limiting factor for remote sensing analyses in our study area (Figure S2), though a strength of the PlanetScope constellation and Sentinel-2 imagery is a high revisit rate of both systems. The Planet constellation has a near daily revisit rate (Roy et al., 2021), while two Sentinel-2 satellites operate with a 5-day repeat interval. This frequency should have provided a greater chance of capturing a clear sky window while the desired phenological conditions are present; however, in reality, there were minimal opportunities to get relatively cloud free imagery during early summer peak NDVI periods to create a maximum dNDVI, for example (Figure S2).

Our use of NExR and dNExR data in the classification of cheatgrass utilize a lesser studied aspect of cheatgrass phenology by capitalizing on the redness of cheatgrass during peak summer periods where cloud free imagery is more prevalent for our mountainous region (Fig. 2, S2). Similar work by Mahood et al. (2023) used the normalized difference senesced vegetation index (NDSVI) as a complement to NDVI to detect senesced annual grass cover in Nevada. Many studies rely heavily on NDVI to capture phenology, either from UAS (as reviewed in Villarreal et al. 2025) or from satellites (Bradley and Mustard 2005; Bradley 2014; Boyte et al. 2015). However, by using imagery from mid-summer, rather than late spring, studies trying to classify early season invasives in frequently cloudy areas may have a better chance of observing differences in invasive and native vegetation phenology that can be used in classification. NExR and dNExR may be less important in more arid regions where peak NDVI imagery is not limited by cloud conditions. Another aspect of NExR and dNExR that may help in the classification of cheatgrass in the larger region we are studying (GYE) is helping to overcome false positives generated by dNDVI data. Ground truthing a 2022 dNDVI model in 2023 led to numerous false positives due to senescent ephemeral vegetation having a similar signal to the early green-up and early senescence of cheatgrass. Similarly, arrowleaf balsamroot (*Balsamorhiza sagittata* (Pursh) Nutt.) displays an early green-up and early senescence dNDVI signal like cheatgrass. In both cases, NExR and dNExR can complement NDVI in a classification model to distinguish cheatgrass from other vegetation types.

Classifying cheatgrass

Our model accuracy increased as pixel size decreased, both in the comparison of Sentinel-2 (10 m) versus PlanetScope (3 m) but also with the addition of 10 cm UAS imagery in either case that used PlanetScope or Sentinel-2 imagery. This result was expected and is widely reported in the use of UAS-based imagery (Villarreal et al. 2025). In each of our comparisons, accuracy improved with the addition of UAS imagery. This project demonstrated the utility of very high-resolution imagery despite not having multiple UAS imagery dates to develop dNDVI or dNExR for understanding phenological changes like Weisberg et al. (2021). The fusion of single date UAS imagery in our models effectively functioned as a pan-sharpening of the model results using either PlanetScope or Sentinel-2 imagery. This was evident from the model results using UAS data where individual sagebrush crowns, juniper trees (*Juniperus* sp.), boulders, and large bunchgrasses like basin wildrye (*Leymus cinereus* Scribn. and Merr.) were identifiable but not evident in the PlanetScope or Sentinel classifications. Furthermore, the NDVI and NExR images derived from UAS imagery allow the classification of cheatgrass in the interstitial spaces between other vegetation types like sagebrush.

The fusion of very high-resolution UAS data to complement satellite imagery is still uncommon in the literature (Villarreal et al. 2025), though the resultant increase in accuracy suggests an opportunity for improving models. Further adoption of UAS technology in applied use may be limited by UAS constraints, including flight time and distance, visual

line of sight regulations, landowner permissions, and computational requirements for image processing. However, newer aircraft with vertical take-off and landing (VTOL) capabilities and fixed wing UAS can collect centimeter-resolution multispectral data over hundreds of hectares in a single flight, potentially allowing for high-accuracy UAS-satellite fusion over larger areas.

This study used dNDVI and dNExR as primary inputs due to an a priori understanding of cheatgrass phenology and how to maximize the difference in signal between nearby control and cheatgrass polygons. These data layers are moderately collinear at cheatgrass locations but can also impart different signals or differentiate false positives by using both in a classification framework. Previous cheatgrass remote sensing work has focused primarily on dNDVI (Kokaly 2010a, 2010b; Waller et al. 2018; Villarreal et al. 2019; Bishop et al. 2019; Smith et al. 2023) and adding dNExR enhances the signal for cheatgrass.

The random forest classification method used to predict cheatgrass is an effective but a relatively basic model considering the tremendous recent growth of AI/ML classification techniques (Maxwell et al. 2018; Dahal et al. 2022; Larson and Tuor 2021). We used the random forest model output flexibly as both a regression technique (modeled probability – Fig. 6) and as a classified presence/absence surface of cheatgrass using a threshold of 0.25 (Fig. 5). Further research could help address more sophisticated models to tease more information out of the training, validation, and remote sensing data used in the prediction of cheatgrass, and potentially make marginal gains in accuracy using UAS data, or possibly substantial gains to the base Sentinel-2 or Planet models. However, our simple model with minimal variables reasonably predicted the likelihood of occurrence at the validation points. Land managers can retain the random forest model to keep this analysis within the capabilities of GEE and allow further updates over time and transferability to nearby areas.

An important aspect of using remote sensing for locating invasive species infestations is the limit of detectability. In this study, the best-performing model using UAS data was relatively sensitive to low levels of cheatgrass cover. In Fig. 6, the steep curve of probability vs observed percent cover indicates values as low as 6–15% were successfully detected 86% of the time (6/7 validation points; Fig. 6). This bin of percent cover shows a large variation in modeled probability as would be expected. However, the variation in modeled probability decreases considerably after percent cover values greater than 25% (Fig. 6). Bradley et al. (2018) found a similar relationship between predicted and observed percent cover of cheatgrass, albeit at a much larger scale and with much more variability.

The level of detection managers would find useful for a remotely sensed product to influence their management action is also a function of minimum patch size. Smaller patches are more easily eradicated with less cost and effort but are much harder to detect (Leung et al. 2002). Large areas with low percent cover are far more conspicuous compared to small patches. Most cheatgrass cover in our study area is concentrated around an old area of legacy disturbance from a defunct irrigation canal. We did not explicitly test for a minimum detectable patch size, but there is agreement in many small patches within our flight area (Figs. 3 and 4). Some patches are picked up with 10-m Sentinel-2 data in model 1; subpixel heterogeneity from fine scale UAS data highlights the underlying cheatgrass distribution and how the signal is expressed in coarser scale data. The similarity of model output and landscape metrics between models 1 and 2 is also interesting when considering detectability and capturing the spatial heterogeneity of cheatgrass infestation (Fig. 5, Table 4); while the use of PlanetScope data improved accuracy, the overall patterns of distribution, patch sizes, and edge metrics are very similar between Sentinel-2 and PlanetScope imagery.

High spatial resolution and near daily revisit rate are two aspects of the PlanetScope constellation that are different from other satellite remote sensing platforms that are achieved through the large number of satellites (180) currently orbiting the earth. With that number of different and inexpensive satellites, a tradeoff in spatial and radiometric precision exists, and scenes downloaded from Planet are not always ‘analysis ready’ (Frazier and Hemmingway, 2021). In our use of PlanetScope data, we found that coregistration errors complicated efforts to use scenes without first reducing our AOI, ordering scenes through the Planet API, and passing them through Planet’s coregister tool. Coregistered scenes still required visual inspection to ensure tight coregistration and ensure differenced products (dNDVI and dNExR) show true

differences in phenology rather than small differences in spatial location mixing adjacent vegetation types and introducing noise in the classification. With our fusion of UAS data, some issues surrounding geolocation are minimized; UAS data are driving the fine-scale patterns in detection, while dNDVI and dNExR data at 3 m resolution (or 10 m Sentinel-2 data) are giving a neighborhood phenology signal to the RF model for classification.

Management implications

The early detection of invasive species via UAS and satellite-based remote sensing make these platforms suitable for implementing the Early Detection and Rapid Response (EDRR) framework used by many natural resource management agencies (Reaser et al. 2020). These methods can also expand the spatial and temporal coverage of detection, provide information in near real-time, be used for difficult to access areas, and possibly reduce resources required for field-based monitoring. However, tradeoffs between the required accuracy to inform management decisions and the potential time and expense of UAS operations lead to important questions for management before adopting new technology. A logical next step for this work would scale up UAS results to inform Planet or Sentinel-2 models and expand the area of interest to help managers find unknown areas of potential cheatgrass infestation in Yellowstone National Park. Similar work has used UAS data to train satellite-based models for broader application (Elkind et al. 2019; Solazzo et al. 2018; Page et al. 2022). Planet or Sentinel-2 based remote sensing models that can provide enough information to inform the prioritization of further inventory or discovery, whether by UAS or field investigation could be used by managers to help improve understanding of where to find the highest likelihood of encountering target species. In our study, we show UAS-based methods can classify cheatgrass with great accuracy (up to 94%) even at low levels of infestation (Fig. 6). Enhancing the cost-effectiveness of discovery and eradication of invasive plants will likely continue to be important for integrating UAS methods into landscape ecology and applied research.

Acknowledgment We thank Sherri Renck for helping coordinate permission to fly UAS on the Custer Gallatin National Forest. We are grateful to the many volunteers who contributed data on cheatgrass occurrence. This work utilized PlanetScope imagery made available through the NASA Commercial SmallSat Data Acquisition (CSDA) Program. We thank Taylor Dudunake, Susan McIlroy, Jeff Ziegeweid, and two anonymous reviewers for comments that improved this manuscript.

Author contributions Conceived and designed the analysis JK, MV, JvN, AR, SB, SM. Collected the data JK, MV, JvN, AZ. Contributed data or analysis tools JK, MV, JvN. Performed the analysis JK, MV, JvN. Wrote the paper JK, MV, JvN, SM. All reviewed, commented, and edited the paper

Funding Funding provided by the U.S. Geological Survey Biological Threats and Invasive Species Program, National Land Imaging Program, and Ecosystems Mission Area; and the National Park Service and Greater Yellowstone Coordinating Committee (Agreement #4,500,162,075).

Data availability The datasets generated during the current study (Kreitler et al. 2025) will be made publicly available at time of publication as a data release through the U.S. Geological Survey (https://doi.org/10.5066/P145LKCS).

Declarations

Conflict of interest The authors declare that the research was conducted in the absence of any commercial or financial relationships that could be construed as a potential conflict of interest. Any use of trade, firm, or product names is for descriptive purposes only and does not imply endorsement by the U.S. Government.

Open Access This article is licensed under a Creative Commons Attribution 4.0 International License, which permits use, sharing, adaptation, distribution and reproduction in any medium or format, as long as you give appropriate credit to the original author(s) and the source, provide a link to the Creative Commons licence, and indicate if changes were made. The images or other third party material in this article are included in the article's Creative Commons licence, unless indicated otherwise in a credit line to the material. If material is not included in the article's Creative Commons licence and your intended use is not permitted by statutory regulation or exceeds the permitted use, you will need to obtain permission directly from the copyright holder. To view a copy of this licence, visit http://creativecommons.org/licenses/by/4.0/.

References

Agisoft LLC. (2023). Agisoft Metashape 1.8—Professional edition: Agisoft LLC software, https://www.agisoft.com/downloads/installer/ Accessed September 9th, 2024

Allred BW, Bestelmeyer BT, Boyd CS, Brown C, Davies KW, Duniway MC, Ellsworth LM, Erickson TA, Fuhlendorf SD, Griffiths TV, Jansen V, Jones MO, Karl J, Knight A, Maestas JD, Maynard JJ, McCord SE, Naugle DE, Starns HD, Twidwell D, Uden DR (2021) Improving

Landsat predictions of rangeland fractional cover with multitask learning and uncertainty. Methods Ecol Evol 12(5):841–849
Balch JK, Bradley BA, D'Antonio CM, Gómez-Dans J (2013) Introduced annual grass increases regional fire activity across the arid western USA (1980–2009). Glob Change Biol 19(1):173–183
Barnett DT, Stohlgren TJ, Jarnevich CS, Chong GW, Ericson JA, Davern TR, Simonson SE (2007) The art and science of weed mapping. Environ Monit Assess 132:235–252
BenDor T, Lester TW, Livengood A, Davis A, Yonavjak L (2015) Estimating the size and impact of the ecological restoration economy. PLoS ONE 10:e0128339
Billings, MT Weather Forecast Office, "NOWData - NOAA Online Weather Data". https://www.weather.gov/wrh/Climate?wfo=byz Accessed August 26th, 2024
Bishop TB, Errigo IM (2023) Using sUAV imagery to map litter of invasive annual grass in dry environmental conditions. Ecol Indic 146:109755
Bishop TB, Munson S, Gill RA, Belnap J, Petersen SL, St. Clair SB (2019) Spatiotemporal patterns of cheatgrass invasion in Colorado Plateau National Parks. Landsc Ecol 34:925–941
Booth MS, Caldwell MM, Stark JM (2003) Overlapping resource use in three Great Basin species: implications for community invasibility and vegetation dynamics. J Ecol 91(1):36–48
Boyte SP, Wylie BK, Major DJ, Brown JF (2015) The integration of geophysical and enhanced moderate resolution imaging spectroradiometer normalized difference vegetation index data into a rule-based, piecewise regression-tree model to estimate cheatgrass beginning of spring growth. Int J Digit Earth 8(2):118–132
Bradford JB, Lauenroth WK (2006) Controls over invasion of *Bromus tectorum*: the importance of climate, soil, disturbance and seed availability. J Veg Sci 17(6):693–704
Bradley BA (2009) Regional analysis of the impacts of climate change on cheatgrass invasion shows potential risk and opportunity. Glob Change Biol 15(1):196–208
Bradley BA (2014) Remote detection of invasive plants: a review of spectral, textural and phenological approaches. Biol Invasions 16:1411–1425
Bradley BA, Mustard JF (2005) Identifying land cover variability distinct from land cover change: cheatgrass in the Great Basin. Remote Sens Environ 94(2):204–213
Bradley BA, Curtis CA, Fusco EJ, Abatzoglou JT, Balch JK, Dadashi S, Tuanmu MN (2018) Cheatgrass (*Bromus tectorum*) distribution in the intermountain Western United States and its relationship to fire frequency, seasonality, and ignitions. Biol Invasions 20:1493–1506
Breiman L (2001) Random forests. Mach Learn 45:5–32
Chintanadilok, J., Patel, S., Zhuang, Y., & Singh, A. (2022). Mission planner: An open-source alternative to commercial flight planning software for unmanned aerial systems: Ae576/ae576, 8/2022. *EDIS*, *2022*(4) https://doi.org/10.32473/edis-ae576-2022.
Dahal D, Pastick NJ, Boyte SP, Parajuli S, Oimoen MJ, Megard LJ (2022) Multi-species inference of exotic annual and native perennial grasses in rangelands of the western United States using harmonized Landsat and Sentinel-2 data. Remote Sens 14(4):807
D'Antonio CM, Vitousek PM (1992) Biological invasions by exotic grasses, the grass/fire cycle, and global change. Annu Rev Ecol Syst 23(1):63–87
Elkind K, Sankey TT, Munson SM, Aslan CE (2019) Invasive buffelgrass detection using high-resolution satellite and UAV imagery on Google Earth Engine. Remote Sens Ecol Conserv 5(4):318–331
European Space Agency. (2024). *Sentinel-2A MSI: Multi-Spectral Instrument, Level-2A*. Retrieved 8/2024 from Google Earth Engine: https://developers.google.com/earth-engine/datasets/catalog/COPERNICUS_S2_SR
Frazier AE, Hemingway BL (2021) A technical review of planet smallsat data: Practical considerations for processing and using PlanetScope imagery. Remote Sens 13(19):3930
Gorelick N, Hancher M, Dixon M, Ilyushchenko S, Thau D, Moore R (2017) Google Earth Engine: planetary-scale geospatial analysis for everyone. Remote Sens Environ 202:18–27
Hesselbarth MHK, Sciaini M, With KA, Wiegand K, Nowosad J (2019) landscapemetrics: an open-source R tool to calculate landscape metrics. Ecography 42(10):1648–1657
Huang C-Y, Asner GP (2009) Applications of remote sensing to alien invasive plant studies. Sensors (Basel) 9(6):4869–4889
Keiter RB, Boyce MS (1994) The Greater Yellowstone ecosystem: redefining America's wilderness heritage. Yale University Press
Kokaly RF (2010a) DESI—detection of early-season invasives (software-installation manual and user's guide version 1.0). US Geol Surv Open-File Rep 1302:2010–1302
Kokaly RF (2010b) Detecting cheatgrass on the Colorado Plateau using landsat data: a tutorial for the DESI software. US Geol Surv Open-File Rep 1327:88
Kreitler, J., von Nonn, J., and M.L. Villarreal. (2025) Data for: UAS and high-resolution satellite imagery improve the accuracy of cheatgrass detection across and invaded Yellowstone landscape: US Geological Survey data release, https://doi.org/10.5066/P145LKCS
Larson KB, Tuor AR (2021) Deep learning classification of cheatgrass invasion in the western United States using biophysical and remote sensing data. Remote Sens 13(7):1246
Leung B, Lodge DM, Finnoff D, Shogren JF, Lewis MA, Lamberti G (2002) An ounce of prevention or a pound of cure: bioeconomic risk analysis of invasive species. Proc R Soc Lond B Biol Sci 269(1508):2407–2413
Emlid Ltd, (2024). Emlid docs. https://emlid.com/ Accessed September 9th, 2024.
Mack RN (1981) Invasion of Bromus tectorum L into western North America: an ecological chronicle. Agro-Ecosystems 7(2):145–165
Mack RN, Pyke DA (1983) The demography of *Bromus tectorum*: variation in time and space. J Ecol. https://doi.org/10.2307/2259964
Mahood AL, Koontz MJ, Balch JK (2023) Fuel connectivity, burn severity, and seed bank survivorship drive ecosystem transformation in a semiarid shrubland. Ecology 104(3):e3968

Maxwell AE, Warner TA, Fang F (2018) Implementation of machine-learning classification in remote sensing: an applied review. Int J Remote Sens 39(9):2784–2817

Meyer GE, Neto JC (2008) Verification of color vegetation indices for automated crop imaging applications. Comput Electron Agric 63(2):282–293

Meyer GE, Hindman TW, Laksmi K (1999) Machine vision detection parameters for plant species identification. In Precision Agriculture and Biological Quality. 3543:327–335. https://doi.org/10.1117/12.336896

Nascente JC, Ferreira ME, Nunes GM (2022) Integrated fire management as a renewing agent of native vegetation and inhibitor of invasive plants in vereda habitats: diagnosis by remotely piloted aircraft systems. Remote Sens 14(4):1040

Olliff T, Renkin R, McClure C, Miller P, Price D, Reinhart D, Whipple J (2001) Managing a complex exotic vegetation program in Yellowstone National Park. Western North American Naturalist 61:347–358

Page MT, Perotto-Baldivieso HL, Ortega-S JA et al (2022) Evaluating mesquite distribution using unpiloted aerial vehicles and satellite imagery. Rangel Ecol Manag 83:91–101

Pasquarella, V. J., Brown, C. F., Czerwinski, W., & Rucklidge, W. J. (2023) Comprehensive Quality Assessment of Optical Satellite Imagery Using Weakly Supervised Video Learning. *In Proceedings of the IEEE/CVF Conference on Computer Vision and Pattern Recognition* pp. 2124–2134

Pastick NJ, Dahal D, Wylie BK, Parajuli S, Boyte SP, Wu Z (2020) Characterizing land surface phenology and exotic annual grasses in dryland ecosystems using Landsat and Sentinel-2 data in harmony. Remote Sens 12(4):725

Peeler JL, Smithwick EA (2018) Exploring invasibility with species distribution modeling: how does fire promote cheatgrass (*Bromus tectorum*) invasion within lower montane forests? Divers Distrib 24(9):1308–1320

Planet Labs PBC. (2022). Planet Application Program Interface: In Space for Life on Earth. https://api.planet.com. Accessed September 20, 2024.

QGIS.org, (2024). QGIS Geographic Information System. QGIS Association. http://www.qgis.org Accessed September 9th, 2024.

R Core Team (2024). R: A language and environment for statistical computing. R Foundation for Statistical Computing, Vienna, Austria. URL https://www.R-project.org/.

Reaser JK, Burgiel SW, Kirkey J, Brantley KA, Veatch SD, Burgos-Rodríguez J (2020) The early detection of and rapid response (EDRR) to invasive species: a conceptual framework and federal capacities assessment. Biol Invasions 22:1–19

Rigge M, Homer C, Cleeves L, Meyer DK, Bunde B, Shi H, Xian G, Schell S, Bobo M (2020) Quantifying western US rangelands as fractional components with multi-resolution remote sensing and in situ data. Remote Sens 12(3):412

Roy DP, Huang H, Houborg R, Martins VS (2021) A global analysis of the temporal availability of PlanetScope high spatial resolution multi-spectral imagery. Remote Sens Environ 264:112586

Sandino J, Gonzalez F (2018) A novel approach for invasive weeds and vegetation surveys using UAS and Artificial Intelligence. In 2018 23rd International Conference on Methods & Models in Automation & Robotics (MMAR). https://doi.org/10.1109/MMAR.2018.8485874

Singh KK, Surasinghe TD, Frazier AE (2024) Systematic review and best practices for drone remote sensing of invasive plants. Methods Ecol Evol 15:998–1015

Singh, N., & Glenn, N. F. (2009). Multitemporal spectral analysis for cheatgrass (Bromus tectorum) classification. International Journal of Remote Sensing, 30(13), 3441-3462.

Smith JT, Allred BW, Boyd CS, Davies KW, Jones MO, Kleinhesselink AR, Maestras JD, Morford SL, Naugle DE (2022) The elevational ascent and spread of exotic annual grass dominance in the Great Basin, USA. Divers Distrib 28(1):83–96

Smith TC, Bishop TB, Duniway MC, Villarreal ML, Knight AC, Munson SM, Waller EK, Jensen R, Gill RA (2023) Biophysical factors control invasive annual grass hot spots in the Mojave Desert. Biol Invasions 25(12):3839–3858

Sofaer HR, Jarnevich CS, Buchholtz EK et al (2022) Potential cheatgrass abundance within lightly invaded areas of the Great Basin. Landsc Ecol 37:2607–2618. https://doi.org/10.1007/s10980-022-01487-9

Soil Survey Staff, Natural Resources Conservation Service, United States Department of Agriculture. Web Soil Survey. Available online at https://websoilsurvey.nrcs.usda.gov/. Accessed [02/10/2025].

Solazzo D, Sankey JB, Sankey TT, Munson SM (2018) Mapping and measuring aeolian sand dunes with photogrammetry and LiDAR from unmanned aerial vehicles (UAV) and multispectral satellite imagery on the Paria Plateau, AZ, USA. Geomorphology 319:174–185

Terry TJ, Hardegree SP, Adler PB (2024) Modeling cheatgrass distribution, abundance, and response to climate change as a function of soil microclimate. Ecol Appl. https://doi.org/10.1002/eap.3028

Villarreal ML, Soulard CE, Waller EK (2019) Landsat time series assessment of invasive annual grasses following energy development. Remote Sens 11(21):2553

Villarreal ML, Bishop TT, Sankey TT, Smith WK, Burgess MA, Caughlin T, Gillan JK, Havrilla CA, Huang T, Lebeau R, Norton CL, Sankey JB, Scholl V, Von Nonn J, Yao EH (2025) Applications of Unoccupied Aerial Systems (UAS) in Landscape Ecology: A review of recent research, challenges and emerging opportunities. Landsc Ecol 40(2):43

Waller EK, Villarreal ML, Poitras TB, Nauman TW, Duniway MC (2018) Landsat time series analysis of fractional plant cover changes on abandoned energy development sites. Int J Appl Earth Obs Geoinf 73:407–419

WebODM Authors, WebODM n.d. https://github.com/OpenDroneMap/WebODM/ Accessed September 9th, 2024.

Weisberg PJ, Dilts TE, Greenberg JA, Johnson KN, Pai H, Sladek C, Kratt D, Tyler SW, Ready A (2021) Phenology-based classification of invasive annual grasses to the species level. Remote Sens Environ 263:112568

Wolkovich EM, Cleland EE (2011) The phenology of plant invasions: a community ecology perspective. Front Ecol Environ 9(5):287–294

Zhou Y, Qiu C, Li Y et al (2023) Integrating UAV data to explore the relationship between microtopographic variation and *Spartina alterniflora* expansion during its early

invasion. Ecol Indic. https://doi.org/10.1016/j.ecolind.2023.110633

Zhu X, Meng L, Zhang Y, Weng Q, Morris J (2019) Tidal and meteorological influences on the growth of invasive *Spartina alterniflora*: evidence from UAV remote sensing. Remote Sens 11(10):1208

Publisher's Note Springer Nature remains neutral with regard to jurisdictional claims in published maps and institutional affiliations.